International Journal of Power Electronics and Drive System (IJPEDS)
Vol. 17, No. 2, June 2026, pp. 1165~1176
ISSN: 2088-8694, DOI: 10.11591/ijpeds.v17.i2.pp1165-1176

Enhanced power quality in PV integrated EV fed microgrid using intelligent controller

D. Balasubramanyam, G. G. Raja Sekhar, T. Vijay Muni
Department of Electrical and Electronics Engineering, Koneru Lakshmaiah Education Foundation, Vaddeswaram, India

Article Info

Article history:

Received Feb 5, 2025
Revised Mar 4, 2026
Accepted Apr 23, 2026

Keywords:

Dynamic active power filter
Electric vehicles
Grid-to-vehicle
Harmonic mitigation
Indirect current control
Particle swarm optimization
Power quality
Vehicle-to-grid

ABSTRACT

The need for electric cars (EVs) is steadily rising in the world due to the rise in emissions like CO2 and environmental effects brought on by conventional automobiles. EVs have also transformed the transportation industry. These days, EVs are popular because of their special qualities, which include lower noise pollution, carbon emissions, and operating expenses, as well as the capacity to operate in both grid-to-vehicle (V2G) and vehicle-to-grid (V2G) scenarios. Nevertheless, it affects the power distribution grid in a number of ways. There are various power concerns owing to the introduction of EVs in the distribution system, like instability of voltage, distortions in currents, harmonic distortions, power factor degradation, and fluctuations in voltage. The primary emphasis of this study is on mitigating PQ issues like harmonics produced in the distributed power network when electric vehicles are integrated at the distribution end. In order to reduce harmonics and enhance the distribution side's current profile, a dynamic active power filter (DAPF) with PSO-tuned ICC control technique is introduced. Performance of PSO-DAPF is validated with the help of MATLAB/Simulink, along with V2G and V2G operation.

Corresponding Author:

G. G. Raja Sekhar
Department of Electrical and Electronics Engineering, Koneru Lakshmaiah Education Foundation
Green Fields, Vaddeswaram, Guntur, Andhra Pradesh, India
Email: rsgg73@gmail.com

1. INTRODUCTION

The transition to renewable energy has been the primary focus in recent years due to growing awareness of the depletion of fossil resources. In this sense, the swing to electric vehicles is made possible by the unavoidable changes in the transportation sector. Nearly 5 million electric vehicles (EVs) were introduced worldwide [1]. Maintaining a healthy, emission-free environment depends heavily on electric automobiles. So as to meet the growing demand for EVs worldwide, an increasing number of EV charging (EVC) stations are being built.

India has 1800 EV charging stations as of March 2021 [1]. Numerous EV charging stations are being established to meet the demands of EVs because of their growing market share worldwide. To correct the voltage fluctuation during power generation, EV station will also be helpful as a flexible load that is allied to the microgrid.

Distribution operators must have a real-time monitoring infrastructure to record the conditions of EV chargers and ensure that their grids operate in a safe manner in compliance with power quality requirements [2], [3]. Through smart charging and V2G EV interfaces, flexibility in the electrical system, including system operators, end users, and aggregators, supports in the interfacing of renewable power to

meet demand [4], [5]. Current harmonics are developed in the system by electric vehicles and charging stations, lowering the supply network's power quality [6].

Numerous studies on dynamic active power filter (DAPF) to enhance the distribution network's power quality using various methods have previously been published [7], [8]. This research presents DAPF utilizing particle swarm optimization (PSO) tuned ICC technique to deal with total harmonic distortion (THD), lowering the impact of real-reactive power needs on the microgrid network, considering the drawbacks of other studies published in the past. To lessen the impact of the harmonics microgrid, PSO-DAPF has been simulated using MATLAB/Simulink [9]. Reactive power suppression, harmonic alleviation is source currents, unity power factor (UPF) at the common connecting point (CCP), and real-reactive power delivery to the EV charging stations during grid fluctuations are major targets of the proposed model [10].

Compared with conventional DAPF and PI-based control strategies reported in the literature, the proposed PSO-based intelligent current controller provides faster dynamic response, enhanced harmonic mitigation, and superior PF correction under nonlinear EV charging conditions. Unlike existing works that either address harmonic compensation or reactive power management separately, this study integrates series energy unit (SEU) support, reference current optimization, and four-leg DAPF operation into a unified control architecture capable of maintaining IEEE-519 compliance during both G2V and V2G modes. This combination of PSO optimization, adaptive filtering, and bidirectional EV interfacing has not been simultaneously addressed in previous studies, thereby establishing the key novelty of this work. The considered model is described in the section 2, the PSO-DAPF controlling is illustrated in the section 3, supporting MATLAB results were presented under the 4th Section, and the proposed model is concluded in the final 5th Section.

2. PROPOSED PV FED DAPF EV CHARGING STATION

The research methodology for the proposed PV-fed DAPF integrated EV charging system was carried out systematically through modeling, controller design, simulation, and performance evaluation stages [5]–[7]. Initially, an extensive literature review was conducted to identify challenges related to renewable energy integration, EV charging, and power quality improvement. Based on the identified research gaps, a PV-supported EV charging architecture integrated with DAPF was developed to improve charging efficiency and reduce harmonic distortions.

The overall configuration of the proposed system is shown in Figure 1, which illustrates the power flow among the Solar Energy Unit (SEU), DAPF, utility grid, and EV charging unit. The DAPF is employed to compensate for harmonics, reactive power, and voltage fluctuations generated during EV charging operations, thereby improving overall grid stability [11], [12].

The PV array was mathematically modeled considering irradiation and temperature variations. Figure 2 shows the effect of series resistance on the (a) I-V and (b) P-V characteristics of the PV module. The analysis indicates that higher series resistance reduces output current and power generation capability, affecting system efficiency [13]–[16].

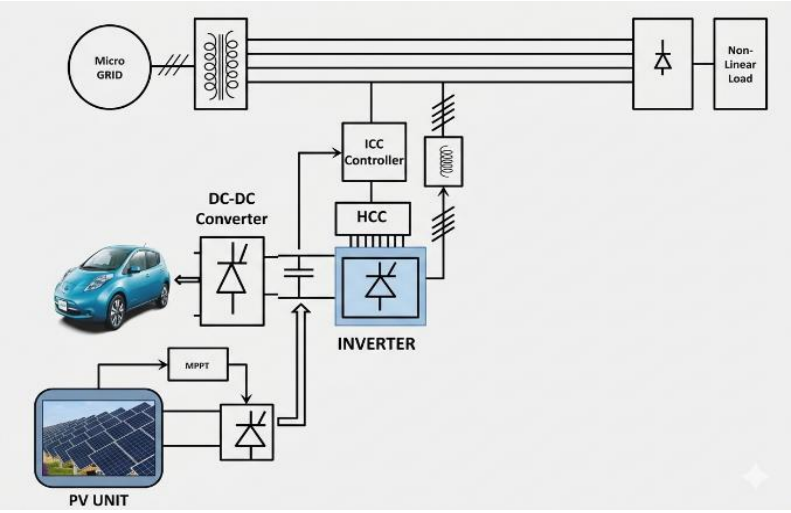

Figure 1. Proposed PV-DAPF fed EV charging station system

2.1. Solar energy unit

In SEU, for higher power point tracking, modified P&O maximum power point tracking (MPPT) is considered [9], and a DC/DC power conditioner is necessary for a stable voltage supply before connecting to a DC link [10], [11]. In this case, the solar unit's MPPT design maximizes output power.

$$P_{PV} = V_{PV} * I_{PV} \quad (1)$$

End solar current and solar voltage of SEU are given by (2) and (3).

$$I_p = I_{sc} - I_{sat}\exp\left[\frac{q}{AkT}\left(V_p + I_p R_{se}\right) - 1\right] - \frac{V_p + I_{sc}R_{se}}{R_{sh}} \quad (2)$$

$$V_p = \frac{AkT}{q}\ln\left\{\frac{I_{sc}}{I_p} + 1\right\} \quad (3)$$

2.2. Electric vehicle charging station

Figure 2 illustrates how an EV charging station is integrated with the grid through a vehicle-to-grid device. To prevent discontinuities in grid power supply and PQ issues, EV charging stations were integrated with DAPF [17]-[19]. The configuration of the EVC station seen in Figure 2, primarily sourced by photovoltaic energy, has a bidirectional converter, which allows power to flow back and forth. By controlling the duty cycle of controllers with a specific frequency and duty ratio, a bidirectional converter controls the voltage [20], [21]. Depending on the situation, the bidirectional converter's buck and boost modes charge and drain the battery in the EVC station by varying firing pulses.

The charging station's control unit creates a duty cycle for the DC/DC converter's PWM generator and employs a P&O MPPT controller to extract the most power possible from the PV cells through DAPF. A PSO controller regulates and controls the DAPF pulses. The MPPT controller draws the most power possible from the source and feeds it to a DAPF converter [22]. A bidirectional inverter receives the converter's output to charge the battery. Based on its pulses, the bidirectional converter alternately charges or discharges.

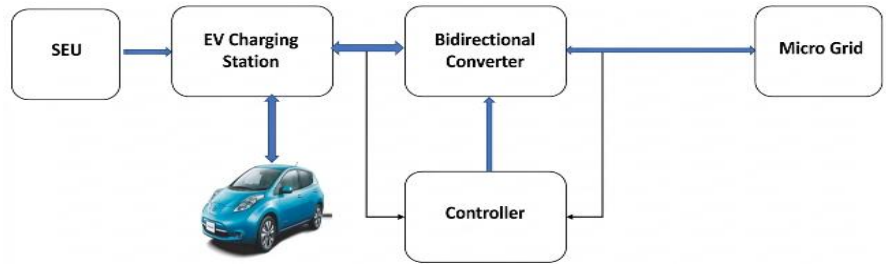

Figure 2. EV charging station

2.3. PSO-DAPF controller

The presented model is a four-wire, three-phase microgrid. Active power can be delivered to or absorbed from the grid by the four-leg inverter. The load's neutral current is compensated by the fourth leg. The inverter's switching mechanism is adjusted so that the combined power of the inverter and load functions as a grid resistor. The battery utilization is replaced by the SEU.

The SEU is connected to the DAPF's DC-link. At CCP, the EVC station and DAPF are integrated at the microgrid source end. The DAPF, which is managed by the PSO- I cosine controller, maintains the power quality. In accordance with the control plan, the DAPF introduces compensating currents. These current balances the necessary amount of reactive power and eliminates the hormone component of the source current. In this case, the inverter absorbs the current harmonics and functions as an inductor [23], [24]. During variations, the necessary quantity of active power is supplied by the integrated SEU at the DAPF's DC link [25].

In a 3ϕsystem, using phase voltages (V_a, V_b, V_c), source RMS value V_m, will be derived using (4).

$$V_m = \{{}^{2}/_{3}\,(V_a^2 + V_b^2 + V_c^2)\}^{1/2} \quad (4)$$

From source voltages, unit vectors will be calculated using (5).

$$W_a = \frac{V_a}{V_m}\, W_b = \frac{V_b}{V_m}\, W_c = \frac{V_c}{V_m} \quad (5)$$

Using unit vectors, in-phase reference currents are computed using (6).

$$I_{das} = I_{ds} * W_a^* \; I_{dbs} = I_{ds} * W_b^* \; I_{dcs} = I_{ds} * W_c^* \quad (6)$$

$$I_{ds} = I_{mds} + I_{cos} \quad (7)$$

$$I_{cos} = \frac{I_a COS\theta_a + I_b \, COS\theta_b + I_c \, COS \, \theta_c}{3} \quad (8)$$

Where I_{mds} is the active component obtained from the PI controller, which can be derived using (9),

$$I_{mdsi} = I_{mds(i-1)} + K_{pVdc}\left(V_{dcei} - V_{dce(i-1)}\right) + K_{IVdc} V_{dcei} \quad (9)$$

here, I_m is phase filtered voltages are proportional to a constant, and the DC link error is V_{dce}. This, in turn, causes the grid current to be sinusoidal.

2.4. Proposed control strategy

As seen in Figure 3, the suggested model makes use of the I cosine PSO controller. Both sinusoidal components of the supply currents (IacosL, IbcosL, IccosL, Iasiṇ, Ibsiṇ, & Icsiṇ) are produced from the source voltages (Vabcs) and source currents (Iabcs). The detailed structure of the PSO-ICC control method used to generate reference currents is presented in Figure 3.

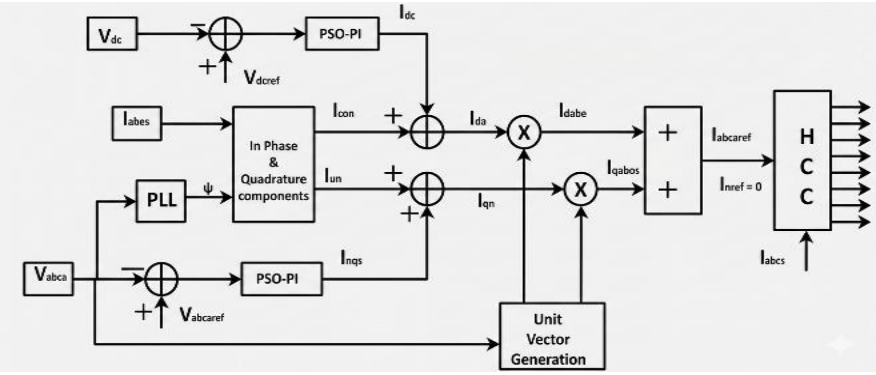

Figure 3. PSO-ICC controller

Both source and DC link voltage regulation are carried out by the control algorithm. Vdc regulation will carry the active power transformer between the grid and SEU, resulting in a current I.Ids are produced when this I_m is coupled with the source current's in-phase component. Idabcs, the direct component of reference current, will be produced by multiplying this Ids by the unit vectors W_a, W_b, and W_c. Iqabcs. Quadrature component of reference currents is also produced following source voltage control and unit vector multiplication. Additionally, the Idabcs and Iqabcs of source currents are added to create the reference currents Iaref, Ibref, and Icref. Inref = 0 will be used to represent the neutral reference current.

In this model, I use cosine PSO-controlled DAPF to compensate for harmonics injected by the EVC station and the reactive power required at the CCP. The PSO controller receives the deviation between the DC link and reference voltages. This discrepancy is smoothed by the PSO controller, which then transmits the signal for the creation of the reference current. In a similar manner, the bottom PSO controller receives the deviation between the actual source voltage and the reference voltage, processes the error signal, and outputs reference currents. This takes into account both source and DC link voltage disturbances.

The quadrature components are derived from (10).

$$I_{qas} = I_{qs} * W_a^* \, , I_{qbs} = I_{qs} * W_b^* , I_{qcs} = I_{qs} * W_c^* \quad (10)$$

Where:

$$I_{qs} = I_{mqs} + I_{sin} \quad (11)$$

$$I_{sin} = \frac{I_a Sin\theta_a + I_b \, Sin\theta_b + I_c \, Sin \, \theta_c}{3} \quad (12)$$

From (6) and (10) net reference currents generated are given by (13) to (15).

$$I_{asref} = I_{das} + I_{qas} \quad (13)$$

$$I_{bsref} = I_{dbs} + I_{qbs} \quad (14)$$

$$I_{csref} = I_{dcs} + I_{qcs} \quad (15)$$

The hysteresis current controller (HCC) is now supplied by the deviation between actual and reference currents. This deviation is used by HCC to create the pulses to DAPF [10]. Phase-A's switching function is provided in the DAPF.

$$HB < (I_a^* - I_a) \rightarrow S_A = 1 \text{ and}$$
$$HB > (I_a^* - I_a) \rightarrow S_A = 0 \quad (16)$$

An evolutionary computation technique called particle swarm optimization mimics the social behavior of swarms, such as groups of birds searching for food in a certain area. The PSO method looks for the best solution for the fitness (objective) function in space. It assesses itself according to the mobility of each particle and the cooperation of the swarm. Depending on the swarm's experience and best understanding, each particle moves at random. It travels in the direction of its best fit, X_{pb}, and current best global fit, X_{gb}. The implemented PSO method is displayed in Figure 4. The PSO algorithm's fundamental guidelines are as follows: i) Best fitness and global best position are updated; ii) Each particle's velocity and position are updated; and iii) Each particle's fitness value is evaluated.

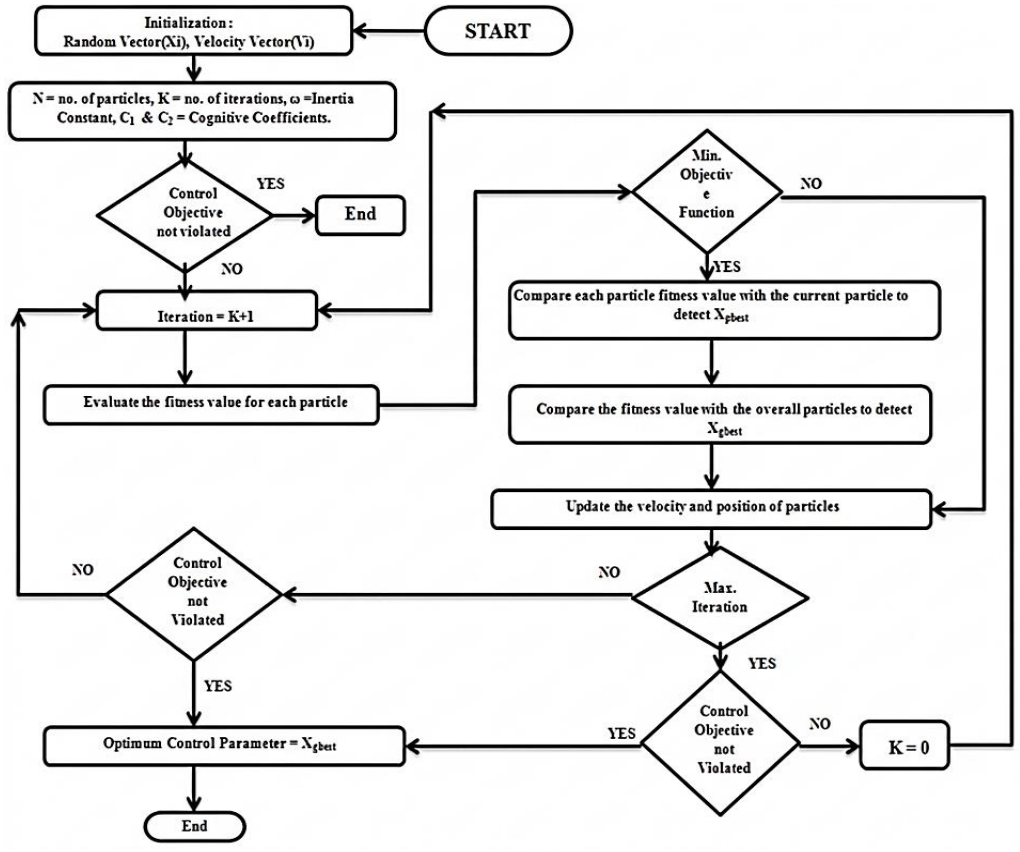

Figure 4. PSO algorithm

Let velocity vector be Vi=[vi1, vi2,… vin] and position vector is Xi=[xi1, xi2,.. xin] in search space. Each particle's velocity and position are updated using (17) and (18).

$$V_i^{k+1} = w.V_i^k + c_1 . r_1 \left[X_{pb}^k - X_i^k\right] + c_2 . r_2 \left[X_{gb}^k - X_i^k\right] \quad (17)$$

$$X_i^{k+1} = X_i^k + V_i^{k+1} \quad (18)$$

Where w is the inertia, r_1 and r_2 are random values, c_1 and c_2 are coefficients. The initialization values for the PSO algorithm are shown in Table 1.

To enhance the technical rigor of this work, the proposed PSO-based DAPF controller is now described in greater detail, including mathematical modeling, reference current computation, PSO optimization criteria, and DC-link voltage regulation. Additional simulation analysis and comparison with conventional DAPF and PI-based controllers have been included to clearly demonstrate the superior dynamic response, harmonic suppression capability, and power factor correction achieved by the proposed control scheme

Table 1. Initialization values of PSO

Feature	Initialization	Feature	Initialization
W (Inertia)	0.7	V_{max}, V_{min}	1, -1
C_1, C_2	1, 0	Swarm size	40
Fitness	1		

3. SIMULATION RESULTS

Using MATLAB/Simulink, the proposed Icosine PSO-controlled DAPF is simulated. Here, two renewable energy sources are efficiently linked to the grid. SEU is connected to the grid via DAPF rather than directly, which has several benefits.

3.1. Current profile

The primary cause of harmonics in the grid current is the EVC station. Figure 5 shows the source, load, and injected currents in Phase A. Before 0.1 s, the source current is distorted due to the EV charger. After the PSO-DAPF is activated, a compensating current is injected, and the source current becomes clean and sinusoidal, demonstrating effective harmonic suppression. The source current (Iabcs) has nonlinearities prior to time t = 0.1 sec. Opposing currents injection at CCP reduces the nonlinearities after t = 0.1 sec. when DAPF is operational. Figure 6 presents the three-phase source, load, injected, and SEU currents. The PSO-DAPF provides balanced harmonic compensation across all phases, resulting in smoother, more symmetrical source currents and reduced neutral current.

The current waveforms clearly show that before 0.1 sec, the source current contains substantial distortion due to the nonlinear EV charger. After activation of the PSO-DAPF, the injected compensating current effectively cancels the harmonic components, resulting in a near-sinusoidal source current. This confirms the controller's capability for real-time harmonic compensation. The three-phase current profiles further demonstrate that the proposed system balances unbalanced loads and reduces neutral current, validating the functionality of the four-leg topology.

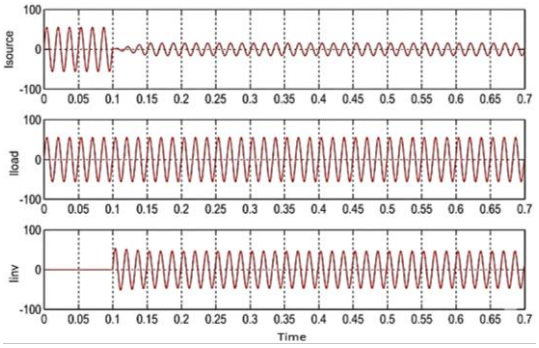

Figure 5. Source-load-injected currents

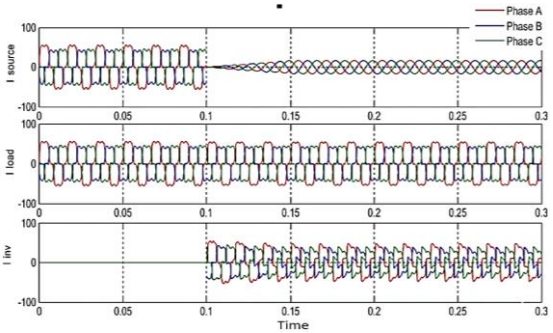

Figure 6. Source-load-injected currents in three phases

3.2. UPF

At t = 0.1 seconds, the DAPF is connected. Before this point, there is a phase deviation in both voltage and current. When DAPF is active, both current and voltages are in phase due to the suppression of reactive power at CCP. During DAPF activation, the grid delivers zero reactive power, and the required reactive power is supplied by DAPF at CCP. This, in turn, leads to UPF. Stated PQ standards are achieved. Figure 7 shows the alignment of source voltage and source current after DAPF activation. The previously

lagging current becomes in-phase with the voltage, confirming unity power factor and proper reactive power compensation at the CCP. The variation in power factor before and after activation of the PSO-DAPF is illustrated in Figure 8, highlighting the achievement of UPF at the CCP.

Before the DAPF operation, the source current lags the voltage due to the reactive power drawn by the EV charging station. With the PSO-DAPF active, the voltage and current become aligned, achieving a unity power factor (PF=1). The PF curve in Figure 8 confirms the complete elimination of reactive power demand at the CCP. This directly supports the claim that the proposed controller improves voltage–current synchronization and overall power quality.

The PSO-DAPF dynamically delivers the reactive power required by the EV charging station. Figure 9 shows that the SEU-fed DAPF injects both active and reactive power during grid fluctuations, reducing the burden on the grid. This behavior validates the dual role of the DAPF as both a harmonic compensator and a reactive power regulator.

3.3. Reactive power compensation

SEU-fed DAPF provides the reactive power required at the CCP by the EVC station. In this case, the DAPF injects both active powers generated by SEU and the necessary reactive power. Thus, without the need for extra power conditioning equipment, the suggested DAPF operates with power quality and uses an active power injector from SEU. Real power delivery to the EVC station and reactive power delivery. Figure 9 presents the required real and reactive power injection from SEU-DAPF.

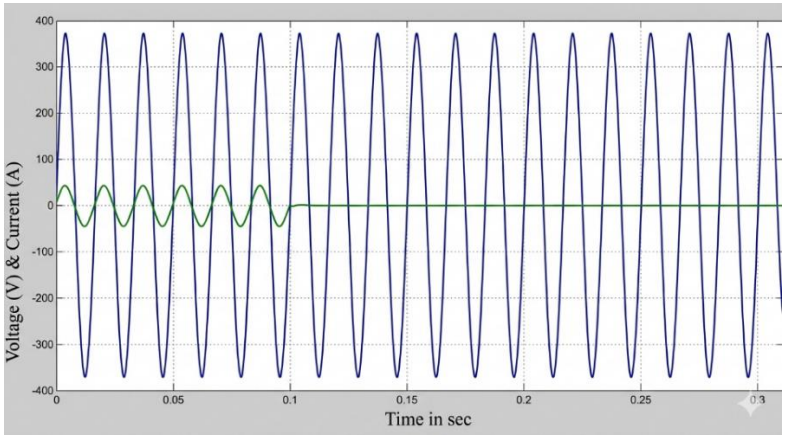

Figure 7. In phase source voltage – current

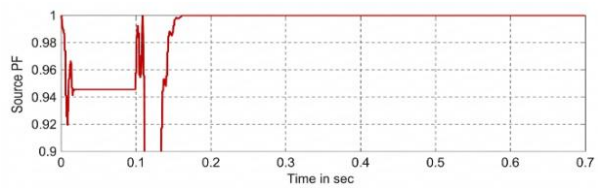

Figure 8. Power factor before & after PSO-DAPF

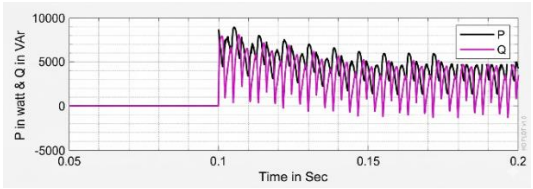

Figure 9. Required real & reactive power injection from SEU-DAPF

3.4. Harmonic suppression at CCP

Under various scenarios, harmonic suppression is examined. They have ANFIS-DAPF and lack DAPF.

- Case 1: Figure 10 displays the current source's THD percentage without DAPF. Because of the EVC station, the percentage THD is higher in the three source currents.
- Case 2: At t = 0.1 seconds, PSO-DAPF is activated at CCP. Source currents % THD with PSO tuned DAPF is displayed in Figure 11. According to IEEE standards, %THD must be below 5%. Here, decreased source current %THD achieved harmonic cancellation below 4%.

The THD results demonstrate significant improvement. Without compensation, the source current THD exceeds IEEE-519 limits (>19–26%). After PSO-DAPF activation, THD drops below 4%, meeting standard requirements. The comparative values in Table 2 confirm that the PSO-DAPF outperforms both the

PI-based and uncompensated cases. This provides strong support for the claim that the proposed intelligent controller offers superior harmonic mitigation.

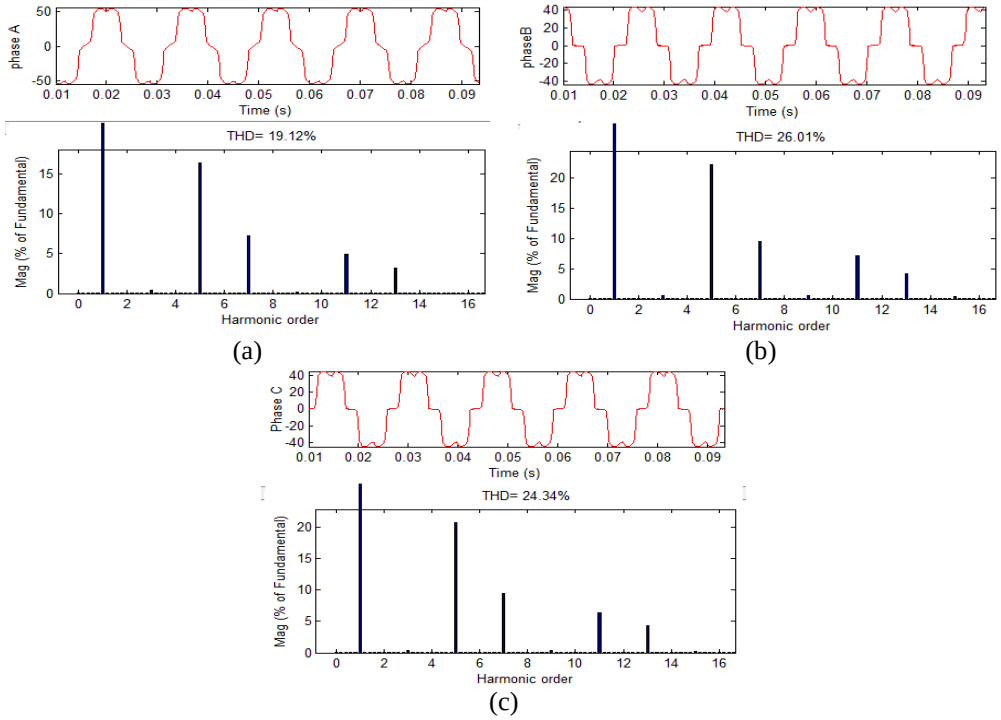

Figure 10. Harmonic disturbances in supply currents in the absence of PSO-DAPF (<0.1s)

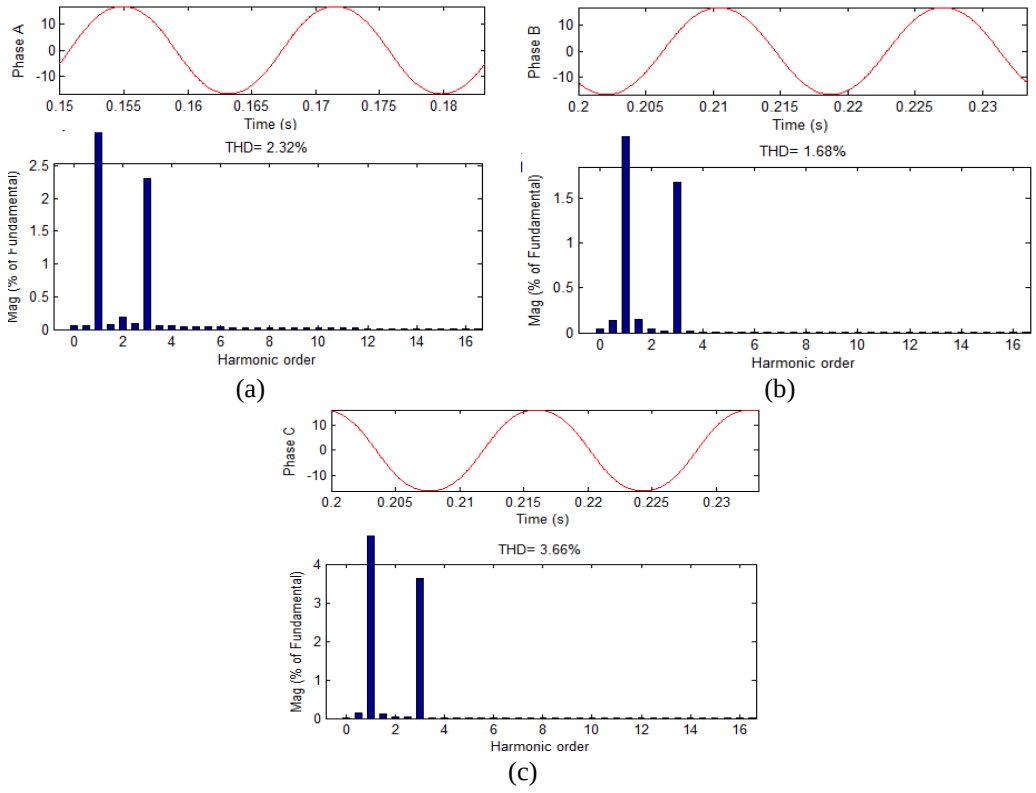

Figure 11. Harmonic disturbances in supply currents in the absence of PSO-DAPF (>0.1s)

In contrast to existing DAPF and PI-controlled systems, the proposed PSO-DAPF achieves a significantly lower THD (<4%), maintains unity PF under all loading conditions, and provides stable reactive power support. Previous studies have shown limitations such as slow dynamic response, higher residual harmonics, or unstable operation during G2V/V2G transitions. The present work demonstrates that PSO-based current optimization and SEU-assisted filtering effectively overcome these limitations, offering improved waveform quality and better compliance with IEEE-519 standards.

Figure 12 illustrates the system performance during grid-to-vehicle (G2V) operation, where the DC-bus voltage and AC-side voltage/current waveforms demonstrate stable and efficient EV battery charging. The DC-link voltage remains regulated with minimal fluctuations, indicating effective converter control and balanced power transfer. In addition, the AC-side waveforms remain smooth and synchronized, confirming good power quality and reliable charging performance under G2V mode.

Figure 13 presents the vehicle-to-grid (V2G) operation, where the EV battery supplies power back to the utility grid through controlled discharging. The AC-side current reverses direction while maintaining synchronization with the grid voltage, demonstrating successful bidirectional power flow. The stable DC-bus and smooth AC-side waveforms validate the effectiveness of the proposed control strategy in ensuring reliable energy transfer and grid support during V2G operation

Table 2. Parameters considered for the proposed model

S.No	Quantities	Specifications
1	Grid voltage	380 V and 50 HZ
2	DC link voltage	Vdc = 300 V C = 3000 µF
3	Solar energy unit	35 v, 8 A, 4.5 KW
4	EVC station	(A-N) R = 26.66 ohms, L = 12 mH & (C-N) R = 36.66 ohms L = 10 mH
5	Impedances	Zs = 0.05 mH Rl = 0.02 ohms Xl = 0.1 mH

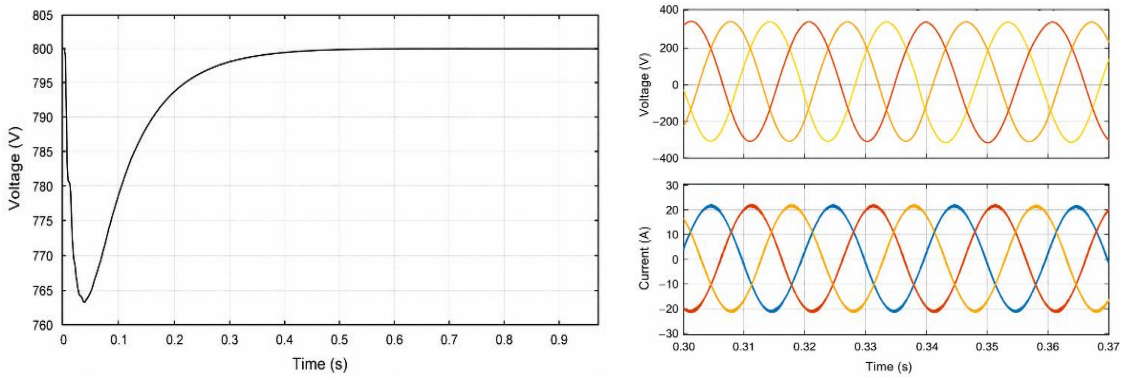

Figure 12. G2V Operation-DC bus & AC side voltages and currents

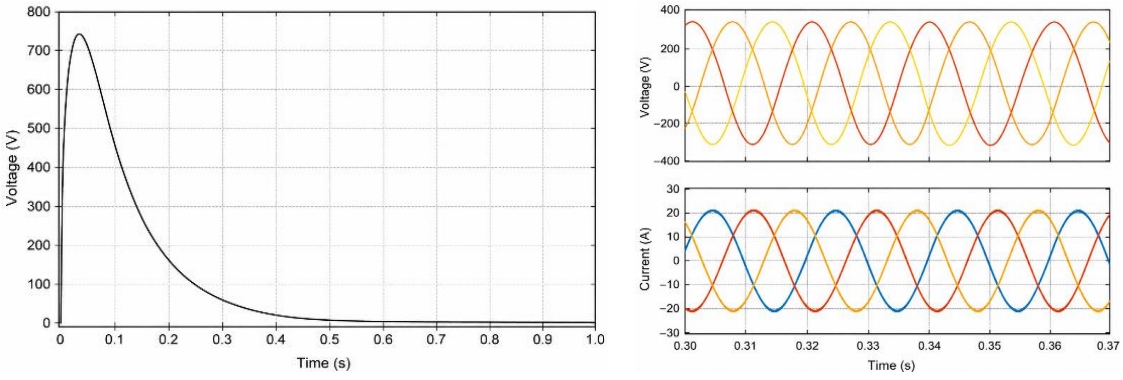

Figure 13. V2G operation-DC bus & AC side voltages and currents

The proposed system maintains stable operation during G2V and V2G transitions. Figure 12 shows smooth DC-link voltage and controlled AC-side currents during G2V charging. Figure 13 illustrates the controlled power flow from EV to the grid during V2G discharge. These results support the claim that the system ensures continuous power flow and maintains PQ standards under both operating modes. It is evident from Table 3 that PSO-DAPF successfully alleviates the harmonics at the grid's CCP.

Table 3. Parameters considered for the proposed model

Parameter	Absence of DAPF	Activation with PI-DAPF	Activation with PSO-DAPF
PF	0.95	1	1
		THD	
Ia	19.1	2.3	2.3
Ib	26	1.7	1.6
Ic	24.3	3.6	3.6

4. CONCLUSION

This research presents a model that effectively accounts for the reactive power required at CCP and reduces harmonics. I cosine PSO-controlled DAPF successfully lowers the %THD of source current to a significant level, as demonstrated by comparison with other conventional techniques. The model gives the load supply continuity. From the solar unit attached to DAPF's DC link end, the presented system provides the active power required under grid disturbances.

The simulation results confirm that the proposed model effectively performs multiple power quality improvement functions under various operating conditions. The DAPF successfully provides reactive power compensation at the common coupling point (CCP), which helps in maintaining voltage stability and reducing reactive power demand from the grid. The system also achieves unity power factor (UPF) at the CCP, ensuring efficient power transfer and minimizing energy losses. In addition, the source current waveforms show a considerable reduction in total harmonic distortion (%THD), demonstrating the effectiveness of the proposed control strategy in harmonic mitigation and power quality enhancement. The results further indicate that the electric vehicle charging (EVC) station receives active power from the solar energy unit (SEU) through the DAPF, eliminating the need for additional power converters and thereby reducing system complexity and cost.

Compared with existing approaches, the proposed method provides better harmonic suppression, faster transient response, and improved overall power quality during bidirectional EV operation. The system maintains stable operation during both charging and discharging modes, ensuring reliable power exchange between the EV, grid, and renewable energy source. These results demonstrate that the proposed technique offers superior performance over conventional DAPF and intelligent-control methods reported in recent studies.

FUNDING INFORMATION

This research was supported by Koneru Lakshmaiah Education Foundation, Science and Engineering Board, Department of Science and Technology (DST) (EEQ/2023/000744).

AUTHOR CONTRIBUTIONS STATEMENT

This journal uses the Contributor Roles Taxonomy (CRediT) to recognize individual author contributions, reduce authorship disputes, and facilitate collaboration.

Name of Author	C	M	So	Va	Fo	I	R	D	O	E	Vi	Su	P	Fu
D. Balasubramanyam	✓	✓	✓	✓	✓	✓		✓	✓	✓			✓	
G. G. Raja Sekhar		✓				✓		✓	✓	✓	✓	✓		
T. Vijay Muni	✓		✓	✓	✓		✓			✓	✓		✓	✓

C : **C**onceptualization
M : **M**ethodology
So : **So**ftware
Va : **Va**lidation
Fo : **Fo**rmal analysis
I : **I**nvestigation
R : **R**esources
D : **D**ata Curation
O : Writing - **O**riginal Draft
E : Writing - Review & **E**diting
Vi : **Vi**sualization
Su : **Su**pervision
P : **P**roject administration
Fu : **Fu**nding acquisition

CONFLICT OF INTEREST STATEMENT

Authors state no conflict of interest.

DATA AVAILABILITY

Data availability is not applicable to this paper as no new data were created or analyzed in this study.

REFERENCES

[1] R. Uthra, D. Suchitra, T. S. Babu, and B. Aljafari, "Fuzzy-based EV charging station and DVR-fed voltage compensation for a DFIG-fed wind energy system during grid faults," *International Transactions on Electrical Energy Systems*, vol. 2022, no. 1, p. 1860266, 2022, doi: 10.1155/2022/1860266.

[2] A. Srivastava, M. Manas, and R. K. Dubey, "Electric vehicle integration's impacts on power quality in distribution network and associated mitigation measures: a review," *Journal of Engineering and Applied Science*, vol. 70, no. 1, p. 32, 2023, doi: 10.1186/s44147-023-00193-w.

[3] A. R. Singh *et al.*, "Electric vehicle charging technologies, infrastructure expansion, grid integration strategies, and their role in promoting sustainable e-mobility," *Alexandria Engineering Journal*, vol. 105, pp. 300–330, 2024, doi: 10.1016/j.aej.2024.06.093.

[4] T. V. Muni and S. V. N. L. Lalitha, "Implementation of control strategies for optimum utilization of solar photovoltaic systems with energy storage systems," *International Journal of Renewable Energy Research*, vol. 10, no. 2, pp. 716–726, 2020, doi: 10.20508/ijrer.v10i2.10565.g7943.

[5] M. Patowary, H. H. Alhelou, and G. Panda, "Performance assessment and validation of inverter control current controllers in reduced sensor maximum power point tracking based photovoltaic-grid tied system," *IET Energy Systems Integration*, vol. 4, no. 4, pp. 505–517, 2022, doi: 10.1049/esi2.12076.

[6] K. Dhami and T. S. Saggu, "THD analysis and its mitigation using datacom integrated with EV charging station in the distribution network," *International Journal of Power Electronics and Drive Systems (IJPEDS)*, vol. 15, no. 3, pp. 1990–1997, 2024, doi: 10.11591/ijpeds.v15.i3.pp1990-1997.

[7] M. Rusan, K. Fekete, K. Čvek, and Z. Klaić, "Harmonic impact of EV charging station on prosumer-rich distribution feeders," in *Proceedings of International Conference on Smart Systems and Technologies, SST 2022*, 2022, doi: 10.1109/SST55530.2022.9954770.

[8] D. M. Gado, A. A. A. El-Ela, and S. A. Moussa, "Power quality improvement for electric vehicle using hybrid active power filter," in *ICEEM 2021 - 2nd IEEE International Conference on Electronic Engineering*, 2021, doi: 10.1109/ICEEM52022.2021.9480619.

[9] A. Kazemtarghi, A. Chandwani, N. Ishraq, and A. Mallik, "Active compensation-based harmonic reduction technique to mitigate power quality impacts of EV charging systems," *IEEE Transactions on Transportation Electrification*, vol. 9, no. 1, pp. 1629–1640, 2023, doi: 10.1109/TTE.2022.3183478.

[10] A. Alobaidi, H. Desroches, and M. Mehrtash, "Impact of vehicle to grid technology on distribution grid with two power line filter approaches," in *IEEE Green Technologies Conference*, 2021, pp. 163–168. doi: 10.1109/GreenTech48523.2021.00035.

[11] S. Sanal Kumar, S. Palanivel, and M. S. Kamalesh, "Topology synthesis of coupled inductor based four port dc-dc converter for multi-input pv-battery application with autonomous mode selection," *Scientific Reports*, vol. 14, no. 1, 2024, doi: 10.1038/s41598-024-81219-y.

[12] V. Chaturvedi, S. Z. Ahmed, A. Kumar, and S. Jaiswal, "Power quality improvement of grid-connected EV charging station using dstatcom," in *2022 IEEE Students Conference on Engineering and Systems, SCES 2022*, 2022, pp. 1–5. doi: 10.1109/SCES55490.2022.9887756.

[13] S. Kasa, P. Ramanathan, S. Ramasamy, and D. P. Kothari, "Effective grid interfaced renewable sources with power quality improvement using dynamic active power filter," *International Journal of Electrical Power & Energy Systems*, vol. 82, pp. 150–160, 2016.

[14] M. Rupesh and V. S. Tegampure, "Cascade feedforward neural network and deep neural network controller on photovoltaic system with cascaded multilevel inverters: comparison on standalone and grid integrated system," *Journal of Mechatronics, Electrical Power, and Vehicular Technology*, vol. 13, no. 2, pp. 157–178, 2022, doi: 10.14203/j.mev.2022.v13.157-178.

[15] T. Tadivaka, M. Srikanth, and T. V. Muni, "THD reduction and voltage flicker mitigation in power system based on STACOM," in *2014 International Conference on Information Communication and Embedded Systems, ICICES 2014*, 2015. doi: 10.1109/ICICES.2014.7034161.

[16] A. Bosak, A. Bosak, L. Kulakovskyi, and T. Oboronov, "Impact of EV chargers on total harmonic distortion in the distribution system network," in *2019 IEEE 6th International Conference on Energy Smart Systems, ESS 2019 - Proceedings*, 2019, pp. 329–333, doi: 10.1109/ESS.2019.8764244.

[17] A. Ul-Haq, A. Perwaiz, M. Azhar, and S. Ullah Awan, "Harmonic distortion in distribution system due to single-phase electric vehicle charging," in *Proceedings - 2018 2nd International Conference on Green Energy and Applications, ICGEA 2018*, 2018, pp. 205–209, doi: 10.1109/ICGEA.2018.8356277.

[18] P. Swapna Sai, G. G. Rajasekhar, T. V. Muni, and M. S. Chand, "Power quality and custom power improvement using UPQC," *International Journal of Engineering and Technology (UAE)*, vol. 7, no. 2, pp. 41–43, 2018, doi: 10.14419/ijet.v7i2.20.11742.

[19] M. I. A. Bakar, S. M. Uddin, and M. H. H. Rozlan, "Performance analysis of an open-unified power quality conditioner with fuzzy logic and ANFIS controllers for enhanced PQ in distribution system," *Ain Shams Engineering Journal*, vol. 16, no. 12, 2025, doi: 10.1016/j.asej.2025.103836.

[20] T. V. Muni, S. V. N. L. Lalitha, B. R. Reddy, T. S. Prasad, and K. Sai Mahesh, "Power management system in PV systems with dual battery," *International Journal of Applied Engineering Research*, vol. 12, no. Special Issue 1, pp. 523–529, 2017.

[21] B. N. Harish and U. Surendra, "A review on power quality issues in electric vehicle interfaced distribution system and mitigation techniques," *Indonesian Journal of Electrical Engineering and Computer Science (IJEECS)*, vol. 25, no. 2, pp. 656–665, 2022, doi: 10.11591/ijeecs.v25.i2.pp656-665.

[22] N. Babu P, J. M. Guerrero, P. Siano, R. Peesapati, and G. Panda, "An Improved Adaptive Control Strategy in Grid-Tied PV System With Active Power Filter for Power Quality Enhancement," *IEEE Systems Journal*, vol. 15, no. 2, pp. 2859–2870, Jun. 2021, doi: 10.1109/JSYST.2020.2985164.

[23] I. Harshith, B. P. Raj, G. G. Raja Sekhar, and T. V. Muni, "A novel methodology for single phase transformerless inverter with leakage current elimination for pv systems application," *International Journal of Innovative Technology and Exploring Engineering*, vol. 8, no. 6, pp. 1017–1021, 2019.

[24] P. Barman *et al.*, "Renewable energy integration with electric vehicle technology: a review of the existing smart charging approaches," *Renewable and Sustainable Energy Reviews*, vol. 183, p. 113518, 2023, doi: 10.1016/j.rser.2023.113518.

[25] P. Thanuja, M. Aparna, and R. Mounika, "Intelligent control of UPQC for enhancing power quality in PV-integrated smart grids using ANFIS controller," *International Journal of Advanced Trends in Engineering and Management*, vol. IV, no. 08, 2025, doi: 10.59544/jdhw4983/ijatemv04i08p1.

BIOGRAPHIES OF AUTHORS

D. Balasubramanyam is an associate professor who began his academic career in 2010 at Siddartha Educational Academy Group of Institutions and currently serves as head of the department. He has broad teaching experience in core power system subjects and is a research scholar at KL University. His research focuses on power systems, smart grids, and power quality improvement. He can be contacted at email: balurayofhope@gmail.com.

G. G. Rajasekhar associate professor in the Department of Electrical and Electronics Engineering at K. L. University, Vaddeswaram, with about 25 years of administrative and teaching experience. He holds a B.E. in Electrical and Electronics Engineering from Karnatak University, an M.Tech. in High Voltage Engineering from JNTUH, and a Ph.D. from Acharya Nagarjuna University. He has guided over 50 UG and 10 PG projects and is currently supervising 2 Ph.D. scholars. His contributions include more than 50 research publications (3 SCI and 31 Scopus), 6 national and international patents, and a textbook on Renewable Energy Sources. He has received several accolades, including the best teacher award and the visionary edu-leader of the year 2023. He serves as a reviewer, editor, and editorial board member for various international journals and conferences. His research interests span power systems, high voltage engineering, system operation and control, and renewable energy. He is a senior member of IEEE, a life member of ISTE, and holds 12 additional professional memberships, along with completing 10 online certification courses. He can be contacted at email: rsgg73@gmail.com.

T. Vijay Muni is an assistant professor and researcher with more than 14 years of experience in the Department of Electrical and Electronics Engineering at K L Deemed to be University. He received his B.Tech. degree in Electrical and Electronics Engineering from JNTU Hyderabad, M.Tech. degree in Power and Industrial Drives from JNTUK, Kakinada, and a doctoral degree from K L Deemed to be University. He has authored 6 textbooks on the electrical discipline. He has published over 67 Scopus-indexed articles, 16 Web of Science-indexed articles, and over 15 articles in peer-reviewed journals, and also published 6 patents with two grants. His areas of research include power electronic converters, energy management systems, control of electric power grids, renewable energy systems, and microgrids. He is an active Senior member of IEEE. He can be contacted at email: vijaymuni1986@gmail.com.